JOURNAL OF AIRCRAFT
Vol. 47, No. 2, March–April 2010

Gurney Flaps on Slender and Nonslender Delta Wings

D. I. Greenwell*
City University, London, England EC1V 0HB, United Kingdom

DOI: 10.2514/1.46610

A parametric low-speed wind-tunnel study has been undertaken of the effects of Gurney flap height on the aerodynamic characteristics of delta wings with sweep angles of 40, 60, and 70°. Flap effects on lift and drag are consistent with previous two-dimensional data when wing geometry is accounted for by using the change in zero-lift incidence rather than lift and using the relative flap area rather than flap height. Flap deployment primarily affects the attached-flow potential lift on delta wings, with vortex lift being almost unchanged. Induced-drag factors are considerably reduced as flap height is increased, but this is due to the use of flat-plate models with near-zero leading-edge suction. For control applications, pitch/lift ratios are similar to those for delta wings with conventional trailing-edge flaps, but the trim-drag penalties are much higher. An aft shift in loading associated with Gurney flap deployment leads to large aft movements of the aerodynamic center, which significantly reduces control capability.

Nomenclature

a_0	=	lift-curve slope at zero lift
AR	=	aspect ratio, b^2/S
b	=	wing span
c	=	mean aerodynamic chord
c_r	=	root chord
C_D	=	drag coefficient, D/qS
$C_{D\min}$	=	minimum drag coefficient
C_{DV}	=	vortex (induced) drag coefficient
C_{D0}	=	drag coefficient at zero lift
C_L	=	lift coefficient, L/qS
$C_{L\alpha}$	=	lift-curve slope, $dC_L/d\alpha$
C_M	=	pitching-moment coefficient, M/qcS
C_{M0}	=	pitching-moment coefficient at zero lift
C_N	=	normal force coefficient, N/qS
C_{NP}	=	potential flow component of normal force
C_{NV}	=	vortex lift component of normal force
D	=	drag
h	=	projected flap height (measured from lower surface)
K_P	=	potential lift factor, $\equiv C_{L\alpha}$
K_V	=	vortex lift factor
k	=	induced-drag factor, $(C_D - C_{D\min})\pi \mathrm{AR}/C_L^2$
L	=	lift
q	=	dynamic pressure, $\frac{1}{2}\rho V^2$
q	=	lift increase factor on flap height
S	=	wing area
S_f	=	flap frontal area, hb
t	=	wing thickness
α	=	angle of attack
α_{0L}	=	zero-lift angle of attack
α_{0P}	=	zero-lift angle of attack for potential lift component
α_{0V}	=	zero-lift angle of attack for vortex lift component
Λ	=	leading-edge sweep angle

I. Introduction

Many recent unmanned combat air vehicle (UCAV) and micro air vehicle (MAV) concepts are tailless configurations with delta or diamond wing planforms of relatively low (40–50°) sweep angle. In terms of flow characteristics, these planforms sit between low-aspect-ratio slender delta wings with a leading-edge vortex system over the wing and conventional medium-aspect-ratio swept wings with fully attached flow. The resulting aerodynamic and flight dynamic behavior is complex and still not fully understood, particularly at low Reynolds number [1]. For these tailless configurations, pitch control using conventional trailing-edge flaps causes difficulties due to the coupling of pitching moment with lift. Sellars et al. [2] postulated that using tangential trailing-edge blowing on a delta wing could generate pitching moments without any change in lift, due to the interaction between the potential and vortex lift components. This turned out not to be the case [3], but results presented by Li et al. [4] indicated that a Gurney flap could have favorable pitch control characteristics when applied to a nonslender delta wing. The published data on Gurney flaps on delta wings is of rather limited extent, and somewhat contradictory, so an experimental study was undertaken to clarify the effects of sweep angle on the changes in lift, drag, and pitching moment due to flap deployment.

II. Gurney Flaps Applied to Delta Wings

A Gurney flap is a small trailing-edge flap (typically less than 5% chord), deflected at 60–90° to the chord line. The wake flow behind the flap directly alters the trailing-edge Kutta condition [5], leading to a large lift increment despite its small size (for example, a ΔC_L of ~0.8 for a 5% flap on a 2-D airfoil [6]). There is an associated parasite drag penalty, of the order of the frontal area of the flap, but this is dependent on the flap height relative to the local boundary-layer depth and can be negligible for flaps of 2% height or smaller [7].

The vast majority of experimental and theoretical work on Gurney flaps has been on 2-D airfoils, along with a small number of experimental investigations of medium-aspect-ratio (5–6) rectangular wings. Comparatively little work on delta wings with Gurney flaps has been published, with the literature consisting of three relatively comprehensive data sets presenting lift, drag, and pitching moment [4,8–11], along with a handful of papers reporting more limited results [12–14].

Traub and Galls [8] report on a very thorough study of a number of leading-edge and trailing-edge flap configurations on a 70° delta wing. A thin flat-plate wing model was used, with a thickness/chord ratio t/c_r of 0.38% and a blunt leading edge. Constant-height Gurney flaps with height/chord ratios h/c_r of 0.5 and 0.95% were tested at a Reynolds number based on root chord of 1.12×10^6. Traub and Galls also present a detailed comparison with a range of previous studies on 70° delta wings, giving a high level of confidence in the experimental arrangements and data-reduction procedures. The effects of the 0.95% flap on lift, drag, and pitching moment also correspond very closely to the data presented later in this paper.

Presented as Paper 3468 at the 25th AIAA Applied Aerodynamics Conference, San Francisco, CA, 5–8 June 2006; received 7 August 2009; accepted for publication 29 September 2009.

*Reader in Flight Dynamics, School of Engineering and Mathematical Sciences, Northampton Square; d.greenwell@city.ac.uk.

Buchholz and Tso [9] summarize a project study [10] of a range of larger Gurney flaps on a 60° delta wing. A flat-plate wing model was used, with a thickness/chord of 3% and a 45° lower-surface beveled leading edge. Constant-height flaps with height/chord ratios of 1, 2, 3, and 5% were tested at a Reynolds number based on root chord of 8.6×10^5. However, when the results presented in [9] were compared with previous data for 60° delta wings (e.g., [15]), it became clear that the basic wing lift-curve slope was far too high, by a factor of around +30%. An analysis of the entire data set [16] showed that dividing all lift, drag, and pitching-moment measurements by 1.3 gave a more reasonable agreement with published 60° wing data and with the effects of flap height reported later in this paper. This suggests a possible error in the dynamic pressure measurement; whatever the error source, this data set is clearly unreliable.

Li et al. [4,11] present work on a cropped 40° delta wing in two complementary papers. A flat-plate wing model was used, with a thickness/chord of 1.6% and a 60° symmetric beveled leading-edge. Constant-height flaps with height/chord ratios of 1, 2, 3, and 5% were tested at a Reynolds number based on root chord of 2.5×10^5. When the results presented in [4,11] were compared with previous data for 40° delta wings (e.g., [1,17]), it was noted that the lift-curve slope was too low by a factor of −20% (allowing for taper ratio) and that the aerodynamic center was misplaced. No obvious reason could be found for these discrepancies, so again this data set must be considered unreliable.

Figure 1 illustrates the typical effects of Gurney flap deployment on lift, drag, and pitching moment, using data from the sole remaining reliable and comprehensive data set [8]. Lift at zero incidence C_{L0} and maximum lift $C_{L\max}$ both show a significant increase, along with a small increase in lift-curve slope (Fig. 1a). Zero-lift drag C_{D0} increases, but induced-drag factor k reduces (Fig. 1b), leading to a reduction in maximum lift/drag ratio $(L/D)_{\max}$ and an increase in the lift coefficient for minimum drag (Fig. 1c). Flap deployment gives a nose-down change in zero-lift pitching moment C_{m0}, combined with an aft shift in aerodynamic center (Fig. 1d) as dC_m/dC_L becomes more negative. Pitch/lift ratio $\Delta C_{m0}/\Delta C_{L0}$ is negative and of a similar magnitude to conventional trailing-edge controls.

Most explanations of the effects of Gurney flaps suggest that the change in the trailing-edge Kutta condition due to flap deployment leads to a change in effective camber [18,19]. In addition, the pressure difference between upper and lower surfaces at the trailing edge due to the separated wake of the flap [20] leads to an aft shift in loading and hence to an increase in effective chord [21,22]. The 3-D wing behavior shown in Fig. 1 suggests that both factors are operating. The increase in lift, maximum lift, and nose-down pitching moment are all consistent with an increase in effective camber. However, the drag polar remains symmetric about zero lift, presumably because the increase in drag is due directly to the separated wake flow behind the flap, rather than to an incidence-dependent change in profile drag. The increase in lift-curve slope and aft shift in aerodynamic center are consistent with an increase in effective chord, but the reduction in induced-drag factor is less straightforward. Reference [8] suggests that since the lift-dependent induced drag is equal to $C_L \tan\alpha$ for a flat-plate delta wing with zero leading-edge suction, an increase in lift at fixed incidence leads to a reduction in induced-drag factor.

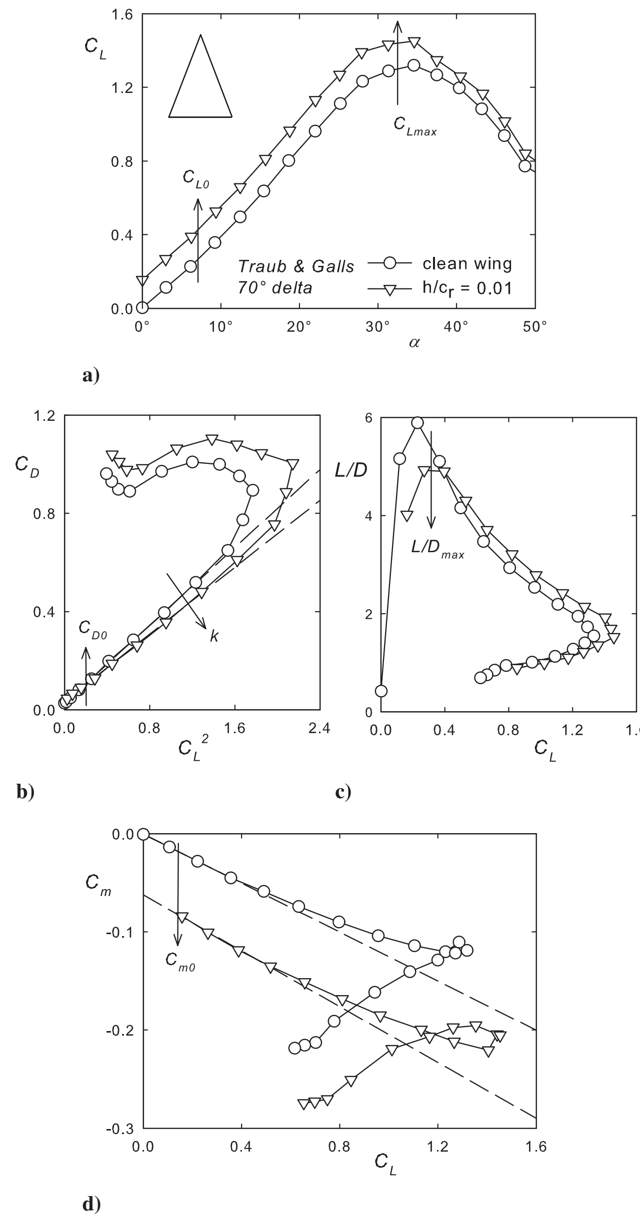

Fig. 1 Typical effects of Gurney flap on delta-wing aerodynamics (data from [1]).

III. Experimental Arrangement

Three sharp-edged flat-plate delta-wing models with leading-edge sweep angles Λ of 40, 60, and 70° were tested in the Bristol University 0.8 × 0.6 m Low-Turbulence Wind Tunnel [23]. This tunnel is of conventional closed-circuit design, with a large contraction ratio and flow control screens to give turbulence levels well below 0.1%. Model planform area S was held constant at 0.072 m^2, giving a model/tunnel area ratio of 0.15 and a root chord c_r of 0.246, 0.353, and 0.436 m, respectively. Models were made of 3 mm aluminum sheet, with leading edges beveled on the lower surface at a 20° included angle (Fig. 2) and with a blunt trailing edge. Flaps were made of 1 mm aluminum sheet and attached to the lower surface of the wing. Forces and moments were measured using an AeroTech 3-component overhead balance, with the models mounted inverted on a single strut plus a pitch pushrod (Fig. 3). A small underwing fairing covered the strut and pushrod attachment points.

Gurney flap heights of 1, 3, and 6% of root chord were tested, with flap height h measured from the wing lower surface. Tests with

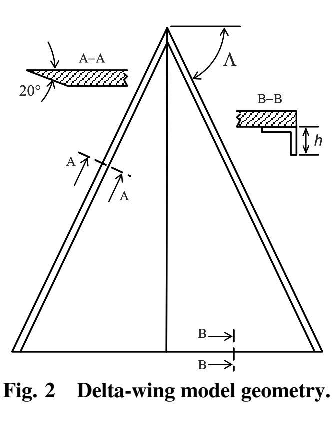

Fig. 2 Delta-wing model geometry.

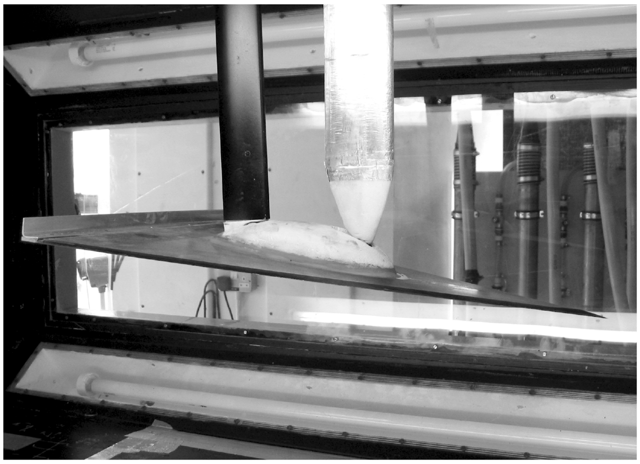

Fig. 3 Model mounted in the Bristol Low-Turbulence Tunnel.

inverted (i.e., upper surface) flaps established that the underwing fairing had no significant effect on trends in aerodynamic behavior with flap height. Tests were carried out at a constant Reynolds number based on root chord of 0.7×10^6. Pitching moments were nondimensionalized using the mean aerodynamic chord c $(2c_r/3)$ and taken about a moment reference center at the quarter-chord point $(0.5c_r)$. Solid and wake blockage were corrected for using the method of [24], with downwash corrections from [25]. Balance accuracy was estimated at better than 0.15% in lift, drag, and pitching moment, with pitch angle set to better than 0.1°. Further details of the experimental arrangement can be found in [26,27].

In order to verify the accuracy of the experimental procedure and data reduction, the baseline delta-wing data was compared with a range of published results for similar wings. Figure 4 compares the basic 60° sweep wing results with data from Flygtekniska Försöksanstalten (FFA) in Sweden [28]. The FFA wing had a very similar geometry (a strut-mounted flat-plate model with an underbody fairing) and was tested at the same Reynolds number of 0.71×10^6. Figure 4 also shows normal force data from the seminal study of delta-wing aerodynamics by Wentz and Kohlman [15] and the theoretical normal force given by the leading-edge suction analogy (LESA) [29]. Angle of attack is given relative to the zero-lift incidence α_{0L}, to allow for the effect of different leading-edge chamfer angles [30] and support interference. Normal force and pitching moments compare very well, with identical lift-curve slopes and aerodynamic centers at low incidence. A similarly good agreement with published data was obtained for the clean 40 and 70° wings and for the 70° wing with a 1% flap [16].

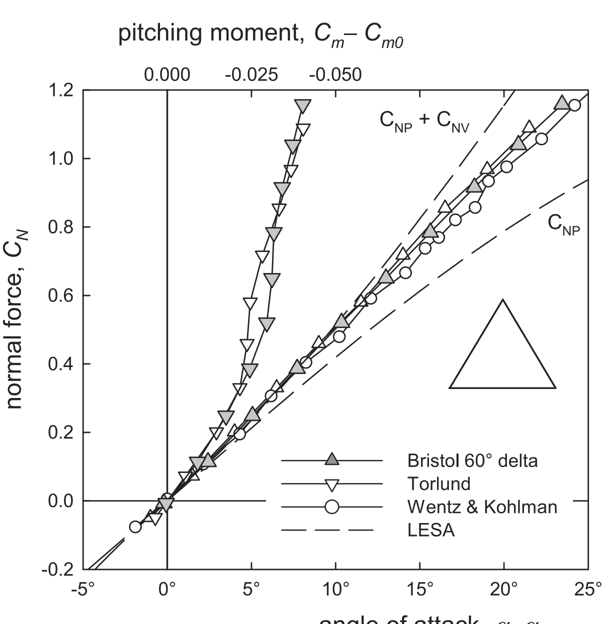

Fig. 4 Comparison of basic 60° wing with theory and results from Torlund [28] and Wentz and Kohlman [15].

IV. Effect of Gurney Flap Height

A. Lift

Looking first at the effect of flap height on lift, Fig. 5 shows the increment in lift coefficient at zero incidence ΔC_{L0} as a function of relative height h/c_r (following previous convention in using the root chord as a reference length for 3-D wing data). The filled symbols denote increments derived from the Bristol data of [26,27], and the open diamond symbols denote a rectangular wing with an aspect ratio of 6 [31]. The crosses show data for a range of 2-D airfoils with Gurney flaps [6,7,32–34]. The same symbols are used in the following figures.

On the basis of thin-airfoil theory, [19] proposes that the lift increment due to a Gurney flap is

$$\Delta C_{L0} = q(h/c)^n \tag{1}$$

where q is supposedly a function of Reynolds number (varying between 2 and 4) and $n = 0.5$. However, plotting the data of [19] and Fig. 5 in log–log form indicates that the variation for both 2-D and 3-D wings is closer to $n = 0.7$ (with q ranging between 3 and 6). The experimental data reviewed in [19] also shows no systematic variation of q with Reynolds number. The difference between the 2-D and 3-D data in Fig. 5 can be attributed to two factors: 1) the effect of aspect ratio on lift-curve slope and 2) the effect of taper ratio on the relative flap height. The effect of variations in lift-curve slope a_0 can be accounted for by replacing lift increment ΔC_{L0} with change in zero-lift incidence $\Delta\alpha_{0L} \approx -\Delta C_{L0}/a_0$. The effect of taper ratio can be accounted for by weighting the flap height by the local chord. For the constant-flap-height data of Fig. 5, the most straightforward weighting method is to use the relative flap area $S_f/S = (hb)/S$. Figure 6 demonstrates that applying both factors collapses the scattered 2-D and 3-D lift increment data of Fig. 5 reasonably well onto a single trend:

$$\Delta\alpha_{0L} \approx 0.9(S_f/S)^{0.7} \tag{2}$$

For the specific case of delta wings, where the lift may be split into potential (or attached) and leading-edge vortex (or separated) flow contributions [29], the question arises as to the relative effect of a Gurney flap on the two lift components. Off-surface flow

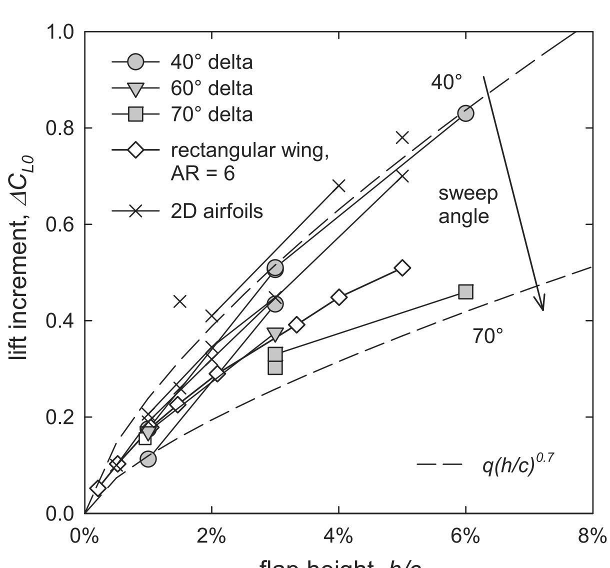

Fig. 5 Effect of flap height on lift increment at zero incidence.

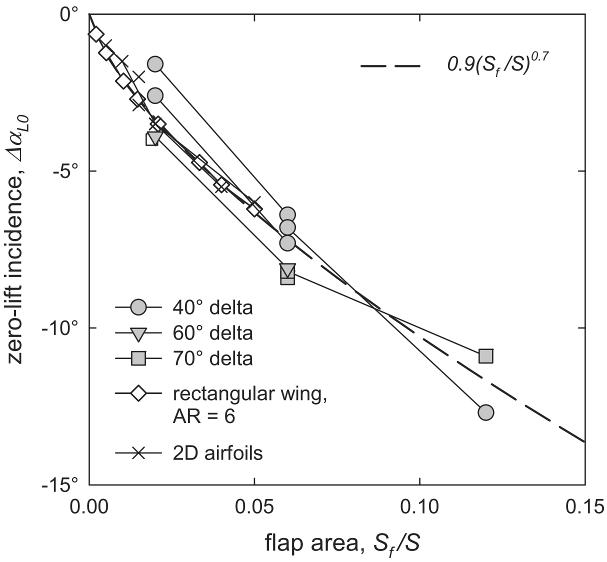

Fig. 6 Effect of flap area on zero-lift incidence.

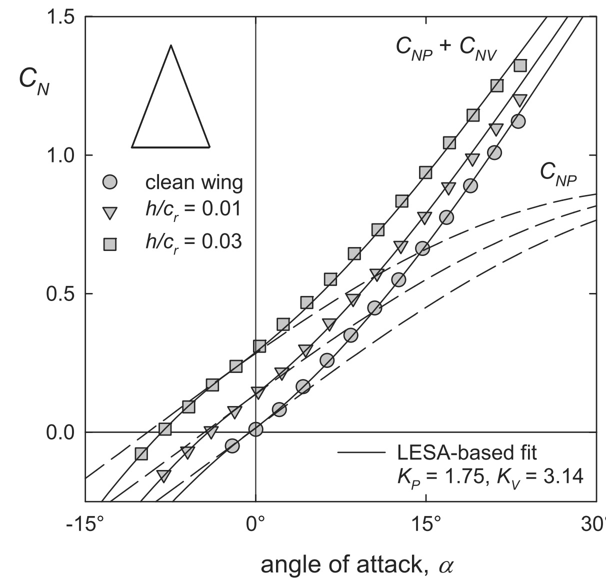

Fig. 7 Effect of Gurney flap height on potential and vortex lift components for a 70° delta wing.

measurements and visualizations reported in [8] indicate that a 1% Gurney flap on a 70° delta wing has a negligible effect on the strength of the primary leading-edge vortex and on the variation of vortex breakdown position with angle of attack, but that the height of the vortex core above the wing surface was reduced slightly. The reduction in vortex height at a given angle of attack would be expected to increase the vortex lift component. An indication of the relative magnitudes of the potential and vortex lift components can be obtained by fitting the LESA lift model [29]

$$C_N = C_{NP} + C_{NV} = K_P \sin(\alpha)\cos(\alpha) + K_V \sin^2(\alpha) \tag{3a}$$

to the experimental normal force data. Following the lead given by Fig. 6, good agreement was obtained by modeling the effects of a Gurney flap as shifts α_{0P} and α_{0V} in the effective incidences of the potential and attached-flow components

$$C_N = K_P \sin(\alpha - \alpha_{0P})\cos(\alpha - \alpha_{0P}) + K_V \sin(\alpha - \alpha_{0V})|\sin(\alpha - \alpha_{0V})| \tag{3b}$$

as demonstrated in Fig. 7. This shows the variation in normal force for a 70° delta wing with 1 and 3% Gurney flaps, compared with Eq. (3b). The corresponding lift factors K_P and K_V and zero-lift offsets α_{0P} and α_{0V}, as determined from a nonlinear least-squares fit to the data, are shown in Table 1. Although the results of fitting a nonlinear equation to experimental data should be treated with caution, it is clear that the Gurney flap has a much greater effect on the potential lift component than on the vortex lift, with the change in zero-lift incidence α_{0P} of the order of six times bigger than the change in the vortex zero-lift incidence α_{0V}. At a given incidence, the change in lift due to flap deployment is largely due to the change in potential lift, with a small contribution from the vortex lift. This is consistent with the results reported in [8]. At low angles of attack, the reduction in local potential lift-curve slope

$$\frac{dC_{NP}}{d\alpha} = K_p \cos(2\alpha)$$

as the potential lift curve moves to the left is counterbalanced by the increase in the vortex lift-curve slope

Table 1 Modified LESA fit to Fig. 7

h/c_r	K_P	K_V	α_{0P}	α_{0V}
0	1.75	3.14	−0.5°	−0.5°
1%	1.75	3.14	−4.5°	−1.0°
3%	1.75	3.14	−9.5°	−2.0°

$$\frac{dC_{NP}}{d\alpha} = K_v \sin(2\alpha)$$

giving a small increase in local lift-curve slope at low incidences.

B. Drag

Figure 8 shows profile drag penalties for 2-D airfoils and 3-D wings as a function of flap height. Plotting the change in minimum drag $\Delta C_{D\min}$ against relative flap area S_f/S collapses 2-D and 3-D data onto a single linear trend. As one might expect for a bluff-body wake flow, the increase in parasite drag area $\Delta D/\frac{1}{2}\rho V^2$ for both 2-D and 3-D wings is approximately equal to the frontal area of the flap hb, giving

$$\frac{\Delta D_{\min}}{\frac{1}{2}\rho V^2} = \Delta C_{D\min} S \approx hb \rightarrow \Delta C_{D\min} \approx \frac{hb}{S} = \frac{S_f}{S} \tag{4}$$

Figure 9 shows that Gurney flap deployment also has a significant impact on induced drag for flat-plate delta wings, due to the loss of leading-edge suction for a sharp-edged wing. Applying the analysis of [8], the lift-dependent drag component of the normal force becomes

$$C_{Di} = C_N \sin(\alpha) = C_L \tan(\alpha) \tag{5}$$

so that the induced-drag factor k is

$$k = \pi \mathrm{AR} \frac{C_{Di}}{C_L^2} = \pi \mathrm{AR} \frac{\tan(\alpha)}{C_L} \tag{6}$$

Since the effect of a Gurney flap on a delta wing is to increase lift C_L at a fixed incidence α, Eq. (6) shows that the corresponding induced-drag factor must reduce as flap height increases. For the LESA model of Eq. (3), the induced-drag factor is a nonlinear function of incidence, with a limiting (maximum) value at zero incidence of

$$k_{\alpha\to 0} = \frac{\pi \mathrm{AR}}{K_P} \tag{7}$$

Equation (7) gives induced-drag factors rather higher than those shown in Fig. 9, due to the effects of nonzero incidence and partial recovery of leading-edge suction, but it does indicate the general effects of wing planform. As sweep angle is reduced, the induced drag increases, because the increased aspect ratio outweighs the effect of increased lift-curve slope.

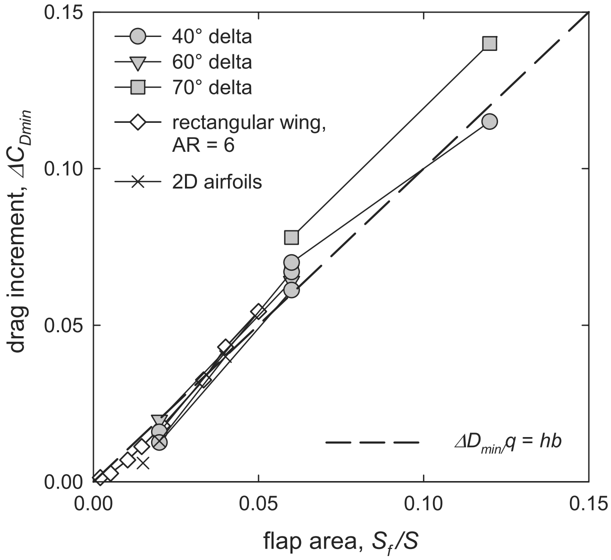

Fig. 8 Effect of flap height on increment in minimum drag.

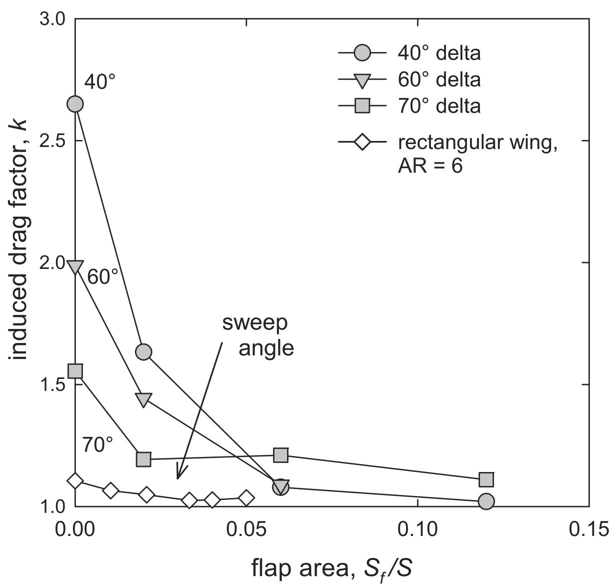

Fig. 9 Effect of flap height on induced-drag factor.

The corresponding effects of flap on lift/drag ratio (e.g., Fig. 1c) follow directly from Fig. 8 and 9, since

$$\left(\frac{L}{D}\right)_{\max} \propto \frac{1}{\sqrt{C_{D0}k}}, \qquad C_{Lmd} \propto \sqrt{\frac{C_{D0}}{k}} \tag{8}$$

The lift coefficient $C_{L,md}$ for maximum L/D ratio increases rapidly with flap deployment, as zero-lift drag C_{D0} increases and induced-drag factor k reduces. The effect on $(L/D)_{\max}$ depends on whether C_{D0} increases more rapidly than k reduces, which in turn depends on the clean-wing profile drag. For the data presented here, $(L/D)_{\max}$ is always reduced by flap deployment.

It should be noted that for practical wings with rounded leading edges, partial recovery of leading-edge suction leads to markedly lower levels of induced drag [35], and so reductions in k due to flap deployment will be much smaller. For example, the rectangular wing with a NACA23012 airfoil section reported in [31] shows very little variation in induced-drag factor with flap deployment. Gurney flaps on a UCAV-type planform with an airfoil cross section are therefore likely to have a much more adverse impact on L/D than that suggested by tests on flat-plate wings [8,10,16].

C. Pitching Moment

The ratio of pitching-moment change to lift change (pitch/lift ratio) is a critical parameter for a control effector on a tailless aircraft. In order to illustrate the effect of wing and flap geometry on this parameter, Fig. 10 plots zero-lift pitching-moment change ΔC_{m0} against change in lift at zero incidence ΔC_{L0} for a range of wings with Gurney flaps (symbols as Fig. 5). Figure 11 shows the corresponding trim-drag penalty $\Delta C_{D\,\min}$ as a function of lift increment.

Two-dimensional thin-airfoil theory gives a limiting maximum value for pitch/lift ratio $\Delta C_{M0}/\Delta C_{L0}$ of -0.25. For 2-D airfoils with Gurney flaps [6,7,32–34], Fig. 10 indicates that the pitch/lift ratio tends to be slightly less than this theoretical value. For 3-D wings with Gurney flaps, the ratio is greater than 2-D theory predicts and increases with reducing aspect ratio up to about -0.35 for a 70° delta. This is the opposite of the trend predicted by [36] for wings with fully attached flow.

For comparison purposes, Fig. 10 also shows pitch/lift ratios for two delta wings with trailing-edge flaps: a 41° delta with a split flap [17] and a 63° delta with a trailing-edge flap [37]. These two wings are not directly comparable with the data reported here, since they had airfoil cross sections and were tested at much higher Reynolds numbers; however, published data for simple delta wings with

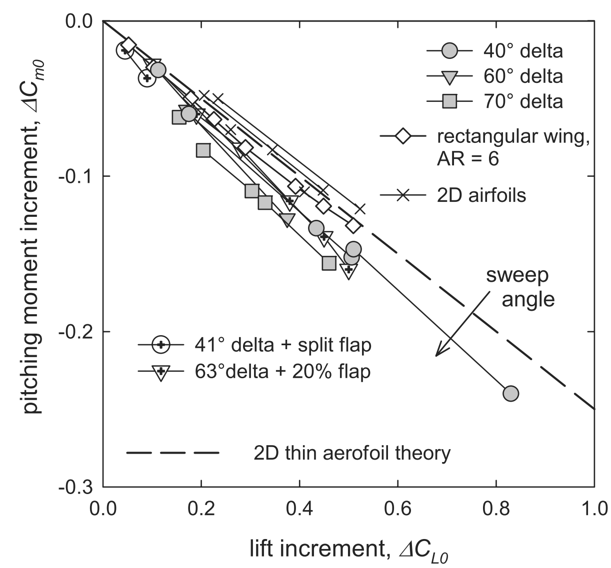

Fig. 10 Pitch/lift ratio for conventional controls and Gurney flaps.

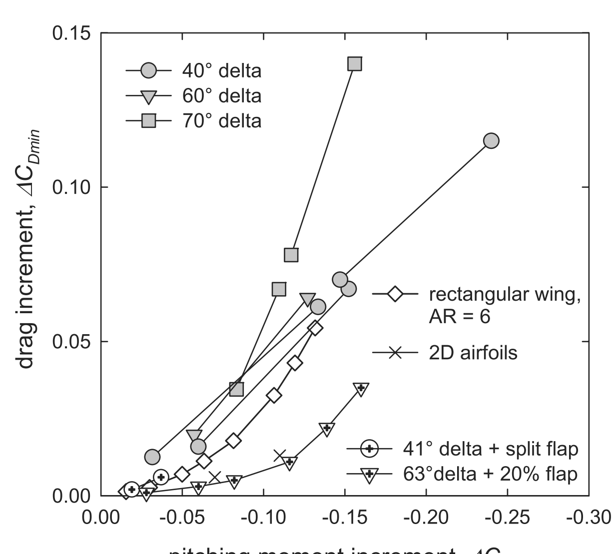

Fig. 11 Trim drag for conventional controls and Gurney flaps.

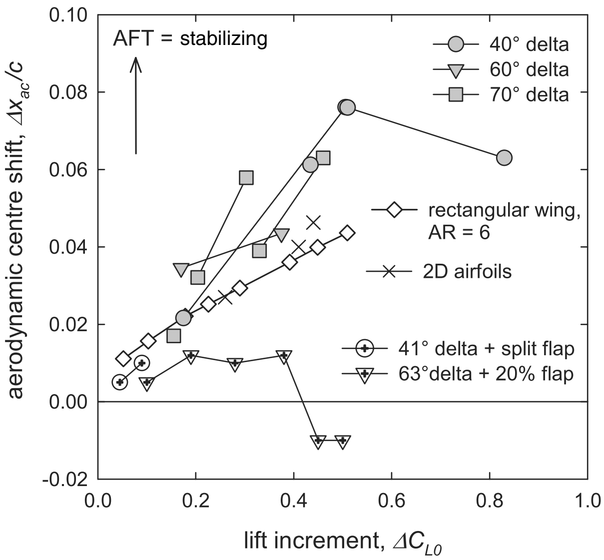

Fig. 12 Aerodynamic-center shift due to Gurney flap deployment.

trailing-edge flaps is remarkably scarce. Bearing in mind the different test conditions, these two data sets indicate that Gurney flaps on delta wings have pitch control characteristics similar to conventional trailing-edge flaps. However, the associated trim drag is on the order of four to five times higher (Fig. 11).

The most significant way in which Gurney flaps differ from conventional trailing-edge controls is in their effect on aerodynamic center, as shown in Fig. 12. For both 2-D and 3-D wings, Gurney flap deployment gives a significant aft shift of the aerodynamic center relative to the clean wing. The magnitude of the shift is roughly proportional to the lift increment. Figure 12 indicates that conventional trailing-edge controls on delta wings can also cause an aft shift in aerodynamic center, but the magnitude is much smaller, and the shift changes sign at higher control deflections. The cause of the aerodynamic-center movement with Gurney flap deployment appears to be an aft shift in chordwise loading distribution, due to the finite pressure difference between the upper and lower surfaces induced by the flap wake at the trailing edge [20].

V. Conclusions

A parametric wind-tunnel study has demonstrated that the effects of Gurney flap deployment on lift, drag, and pitching moment are similar for delta wings with sweep angles of 40, 60, and 70°, spanning vortex flow types from nonslender to slender. The effects of flap height on lift and profile drag are also consistent with the extensive literature on 2-D Gurney flaps, when appropriately parameterized. The influence of wing aspect ratio can be accounted for by using the shift in zero-lift incidence $\Delta\alpha_{0L}$ rather than the increase in lift ΔC_L, while the effect of wing taper can be accounted for by using the relative flap area S_f/S rather than the height/chord ratio h/c_r. Fitting experimental data to the LESA model indicates that on a delta wing the Gurney flap acts primarily to change the zero-lift incidence of the attached-flow potential lift component, with a much smaller effect on the separated-flow vortex lift component. The Gurney flap generates a bluff-body wake, giving an increase in profile drag ΔC_{D0} that is approximately equal to the relative frontal area S_f/S of the flap.

For the simple flat-plate delta-wing models tested here, Gurney flaps give very large improvements in induced drag, which tends to counteract the increase in profile drag due to flap frontal area and hence gives a relatively small reduction in L/D. This is due to the nearly 100% loss of leading-edge suction on a flat-plate wing with a sharp leading edge, which results in unrealistically high induced-drag factors for the clean wings. The induced-drag reduction with flap deployment for a flat-plate wing is essentially a geometry effect, as normal force is increased at a fixed incidence. For practical UCAV and MAV wings with rounded leading edges, the clean-wing induced-drag factors (and hence the relative improvements due to Gurney flap deployment) will be much smaller, and so adverse effects on L/D are likely to be much larger.

Pitch/lift ratios for delta wings with Gurney flaps are similar to those for delta wings with trailing-edge control surfaces and are significantly more negative than for conventional wings with attached flow. Gurney flaps would appear to have a similar pitch control capability to conventional flaps, but this is offset by a much higher trim-drag penalty and by an associated aft (stabilizing) shift of the aerodynamic center.

The usual effective camber explanation of the effects of Gurney flaps on 2-D airfoils has some shortcomings when applied to delta wings. The observed increases in lift, maximum lift, and nose-down pitching moment are all consistent with a change in effective camber. However, the drag polars remain symmetric about zero lift, and the vortex lift component is relatively unaffected. The large aft shift in aerodynamic center is due to the local separated-flow effects near the trailing edge, where the pressure difference between upper and lower surfaces at the trailing edge due to the flap wake leads to an aft shift in loading and hence to an increase in effective chord.

Data comparisons have highlighted a number of issues with the limited literature on delta wings with Gurney flaps. In general, many papers do not clearly specify the moment reference center, the moment reference length, or the point from which flap height is measured, which makes comparisons and assessments of trends very difficult. More specifically, two out of three of the most comprehensive data sets available have lift, drag, and pitching-moment data that are clearly in error, but because no comparison was made with other (readily available) experimental data sets for delta wings, or with simple theoretical predictions, these errors were not recognized before publication.

Acknowledgments

The author wishes to thank Patrick Wichert, Chris Dance, Louise McFarlane, and David Delamore-Sutcliffe for their assistance with the experimental work and data analysis.

References

[1] Gursul, I., Gordnier, R., and Visbal, M., "Unsteady Aerodynamics of Non-Slender Delta Wings," *Progress in Aerospace Sciences*, Vol. 41, No. 7, 2005, pp. 515–557. doi:10.1016/j.paerosci.2005.09.002

[2] Sellars, N. D., Wood, N. J., and Kennaugh, A., "Delta Wing Circulation Control Using the Coanda Effect," AIAA Paper 2002-3269, June 2002.

[3] Harley, C. D., Wilde, P. I. A., and Crowther, W. J., "Application of Circulation Control Manoeuvre Effectors for Three Axis Control of a Tailless Flight Vehicle," AIAA Paper 2009-146, Jan. 2009.

[4] Li, Y. C., Wang, J. J., Tan, G. K., and Zhang, P. F., "Effects of Gurney Flaps on the Lift Enhancement of a Cropped Non-Slender Delta Wing," *Experiments in Fluids*, Vol. 32, No. 1, 2002, pp. 99–105. doi:10.1007/s003480200010

[5] Liebeck, R. H., "Design of Subsonic Airfoils for High Lift," *Journal of Aircraft*, Vol. 15, No. 9, 1978, pp. 547–561. doi:10.2514/3.58406

[6] Gai, S. L., and Palfrey, R., "Influence of Trailing-Edge Flow Control on Airfoil Performance," *Journal of Aircraft*, Vol. 40, No. 2, March–April 2003, pp. 332–337. doi:10.2514/2.3097

[7] Giguere, P., Dumas, G., and Lemay, J., "Gurney Flap Scaling for Optimum Lift-to-Drag Ratio," *AIAA Journal*, Vol. 35, No. 12, Dec. 1997, pp. 1888–1890. doi:10.2514/2.49

[8] Traub, L. W., and Galls, S. F., "Effects of Leading and Trailing Edge Gurney Flaps on a Delta Wing," *Journal of Aircraft*, Vol. 36, No. 4, July–Aug. 1999, pp. 651–658. doi:10.2514/2.2507

[9] Buchholz, M. D., and Tso, J., "Lift Augmentation on Delta Wing with Leading-Edge Fences and Gurney Flap," *Journal of Aircraft*, Vol. 37, No. 6, Nov.–Dec. 2000, pp. 1050–1057. doi:10.2514/2.2710

[10] Buchholz, M. D., "Lift Augmentation on Delta Wing via Leading-Edge

Fences and the Gurney Flap," M.Sc. Thesis, California Polytechnic State University, Dec. 1992.

[11] Li, Y., and Wang, J., "Experimental Studies on the Drag Reduction and Lift Enhancement of a Delta Wing," *Journal of Aircraft*, Vol. 40, No. 2, March–April 2003, pp. 277–281. doi:10.2514/2.3120

[12] Langan, K. J., and Samuels, J. J., "Experimental Investigations of Maneuver Performance Enhancements on an Advanced Fighter/Attack Aircraft," AIAA Paper 1995-0442, Jan. 1995.

[13] Zhan, J., and Wang, J., "Experimental Study on Gurney Flap and Apex Flap on a Delta Wing," *Journal of Aircraft*, Vol. 41, No. 6, Nov.–Dec. 2004, pp. 1379–1383. doi:10.2514/1.4044

[14] Greenblatt, D., Kastantin, Y., Nayeri, C. N., and Paschereit, C. O., "Delta Wing Flow Control Using Dielectric Barrier Discharge Actuators," AIAA Paper 2007-4277, June 2007.

[15] Wentz, W. H., and Kohlman, D. L., "Vortex Breakdown on Slender Sharp-Edged Wings," *Journal of Aircraft*, Vol. 8, No. 3, March 1971, pp. 156–161. doi:10.2514/3.44247

[16] Greenwell, D. I., Dance, C., McFarlane, L., Wichert, P., and Delamore-Sutcliffe, D., "Gurney Flaps on Slender and Non-Slender Delta Wings," AIAA Paper 2006-3568, June 2006.

[17] Demele, F. A., "Effects of a Leading-Edge Slat and a Trailing-Edge Split Flap on the Aerodynamic Characteristics of a Wing –Fuselage Combination Having a Nearly Triangular Wing of Aspect Ratio 2.9 at Mach Numbers from 0.60 to 0.92," NACA RM A57H19, Jan. 1954.

[18] Wang, J. J., Li, Y. C., and Choi, K.-S., "Gurney Flap—Lift Enhancement, Mechanisms and Applications," *Progress in Aerospace Sciences*, Vol. 44, No. 1, 2008, pp. 22–47. doi:10.1016/j.paerosci.2007.10.001

[19] Liu, T., and Montefort, J., "Thin-Airfoil Theoretical Interpretation for Gurney Flap Lift Enhancement," *Journal of Aircraft*, Vol. 44, No. 2, March–April 2007, pp. 667–671. doi:10.2514/1.27680

[20] Jeffreys, D., Zhang, X., and Hurst, D. W., "Aerodynamics of Gurney Flaps on a Single-Element High-Lift Wing," *Journal of Aircraft*, Vol. 37, No. 2, March–April 2000, pp. 295–301. doi:10.2514/2.2593

[21] Traub, L. W., Miller, A. C., and Rediniotis, O., "Preliminary Parametric Study of Gurney-Flap Dependencies," *Journal of Aircraft*, Vol. 43, No. 4, July–Aug. 2006, pp. 1242–1244. doi:10.2514/1.13852

[22] Thompson, B. E., and Lotz, R. D., "Divergent-Trailing-Edge Airfoil Flow," *Journal of Aircraft*, Vol. 33, No. 5, Sept.–Oct. 1996, pp. 950–955. doi:10.2514/3.47040

[23] Barrett, R. V., "Design and Performance of a New Low Turbulence Wind Tunnel at Bristol University," *The Aeronautical Journal*, Vol. 88, No. 873, March 1984, pp. 86–90.

[24] Shindo, S., "Simplified Tunnel Correction Method," *Journal of Aircraft*, Vol. 32, No. 1, Jan. 1995, pp. 210–213. doi:10.2514/3.46705

[25] Pope, A., Rae, W. H., and Barlow, J. B., *Low-Speed Wind Tunnel Testing*, Wiley, New York, 1999.

[26] Wichert, P., "Experimental Investigation of Gurney Flaps on Low Aspect Ratio Delta Wings," M.Sc. Thesis, Univ. of Stuttgart, Stuttgart, Germany, and Univ. of Bristol, Bristol, England, U.K., July 2004.

[27] Dance, C., and McFarlane, L., "Gurney Flaps on Delta Wings," Department of Aerospace Engineering, Univ. of Bristol, Project Rept. 1123, Bristol, England, U.K., May 2005.

[28] Torlund, P.-A., "Wind Tunnel Force Measurements and Visualisation on a 60° Delta Wing in Oscillation, Stepwise Motion and Gusts," *Manoeuvring Aerodynamics*, CP-497, AGARD, Paper 10, Neuilly-sur-Seine, France, May 1991.

[29] Polhamus, E. C., "A Concept of the Vortex Lift of Sharp-Edge Delta Wings Based on a Leading-Edge-Suction Analogy," NASA TN-D-3767, Dec. 1966.

[30] Ericsson, L. E., "Explanation for Huge Differences Between Measurements of Vortex Breakdown on 65° Delta-Wing Configurations," AIAA Paper 1999-1410, Aug. 1999.

[31] Cavanaugh, M. A., Robertson, P., and Mason, W. H., "Wind Tunnel Test of Gurney Flaps and T-Strips on an NACA 23012 Wing," AIAA Paper 2007-4175, June 2007.

[32] Li. Y. C., Wang, J. J., and Zhang, P. F., "Effects of Gurney Flaps on a NACA0012 Airfoil," *Flow, Turbulence and Combustion*, Vol. 68, No. 1, 2002, pp. 27–39. doi:10.1023/A:1015679408150

[33] Myose, R., Papadakis, M., and Heron, I., "Gurney Flap Experiments on Airfoils, Wings and Reflection Plane Models," *Journal of Aircraft*, Vol. 35, No. 2, March–April 1998, pp. 206–211. doi:10.2514/2.2309

[34] Guzel, G., Sankar, L. N., and Rhee, M., "Computational Investigation of the Effects of Gurney Flap on the Aerodynamic Performance of VR-12 Airfoil," AIAA Paper 2005-4960, June 2005.

[35] Carlson, H. W., and Mack, R. J., "Studies of Leading-Edge Thrust Phenomena," *Journal of Aircraft*, Vol. 17, No. 12, Dec. 1980, pp. 890–897. doi:10.2514/3.57981

[36] "Aerofoil and Wing Pitching Moment Coefficient at Zero Angle of Attack Due to Deployment of Trailing-Edge Plain Flaps at Low Speeds," ESDU International, Data Item 98017, Nov. 2003.

[37] Stephenson, J. D., and Amuedo, A. R., "Tests of a Triangular Wing of Aspect Ratio 2 in the Ames 12-Foot Pressure Wind Tunnel 2—The Effectiveness and Hinge Moments of a Constant-Chord Plain Flap," NACA RM A8E03, Sept. 1948.